

Local spin resonance and spin-Peierls-like phase transition in a geometrically frustrated antiferromagnet

S.-H. Lee^{1,2}, C. Broholm^{3,2}, T.H. Kim^{4*}, W. Ratcliff II⁴ and S-W. Cheong^{4,5}

¹ University of Maryland, College Park, Maryland 20742

² NIST Center for Neutron Research, National Institute of Standards and Technology, Gaithersburg, Maryland 20899

³ Department of Physics and Astronomy, The Johns Hopkins University, Baltimore, Maryland 21218

⁴ Department of Physics and Astronomy, Rutgers University, Piscataway, New Jersey 08854

⁵ Bell Laboratories, Lucent Technologies, Murray Hill, New Jersey 07974

Inelastic magnetic neutron scattering reveals a localized spin resonance at 4.5 meV in the ordered phase of the geometrically frustrated cubic antiferromagnet ZnCr_2O_4 . The resonance develops abruptly from quantum critical fluctuations upon cooling through a first order transition to a coplanar antiferromagnet at $T_c = 12.5(5)$ K. We argue that this transition is a three dimensional analogue of the spin-Peierls transition.

PACS numbers: 76.50.+g, 75.40.Gb, 75.50.Ee

It appears that antiferromagnetically interacting Heisenberg spins on the vertices of a lattice of corner-sharing tetrahedra cannot order [1–4]. Characterized by weak connectivity and frustrated interactions [5], this so-called pyrochlore antiferromagnet has no phase transition for spin $S = \infty$ [2,3] and forms a quantum spin liquid with low lying singlet excitations for $S = 1/2$ [4]. Recent experimental [6,7] and theoretical [8,9] work however indicates that small perturbations away from the ideal model can induce low temperature phase transitions. In the quantum critical spin-1/2 antiferromagnetic chain sensitivity to small symmetry breaking perturbations leads to the spin-Peierls transition: A lattice distortion that lowers the energy of the spin system by inducing a gap in the magnetic excitation spectrum. In this letter we report a similar phenomenon for spins on a lattice of corner-sharing tetrahedra.

We examined the spinel antiferromagnet (AFM) ZnCr_2O_4 using neutron scattering. Cubic and paramagnetic at high temperatures, the material undergoes a first order phase transition at $T = 12.5$ K into a tetragonal phase with Néel order. Our measurements and analysis indicate that lattice energy is expended at the phase transition to break the symmetry of frustrated magnetic interactions and thereby select an ordered magnetic phase from a manifold of degenerate states. A local spin resonance develops abruptly below the transition. This resonance is a manifestation of Q -space degeneracy in the ordered phase of a frustrated magnet. Just as the development of a singlet-triplet gap drives the spin Peierls transition, the fact that ordering in a frustrated magnet can push low energy spectral weight into a finite energy resonance plays an important role at the transition in ZnCr_2O_4 .

Cr^{3+} is the source of magnetism in ZnCr_2O_4 . Approximately octahedrally coordinated, the unfilled $3d^3$ shells of these atoms form isotropic $S = 3/2$ degrees of freedom on a lattice of corner-sharing tetrahedra. Assuming that

only nearest neighbor interactions are appreciable yields an estimate of $J = (3k_B\Theta_{CW}/zS(S+1)) = -4.5$ meV for the exchange constant. Here $\Theta_{CW} \approx -390$ K is the Curie-Weiss temperature derived from high temperature susceptibility data [5] and $z = 6$ is the nearest neighbor coordination number. Experiments on Cr^{3+} pairs in ZnGa_2O_4 [10,11] give values for J ranging from -2.8 meV to -4.0 meV and also provide evidence for biquadratic exchange $\mathcal{H}_2 = j(\mathbf{S}_1 \cdot \mathbf{S}_2)^2$ with $j = -0.21(4)$ meV.

A 25 g powder sample was prepared by solid state reaction between stoichiometric amounts of Cr_2O_3 and ZnO in air. Rietveld analysis of neutron powder diffraction data from the NIST BT1 diffractometer shows that ZnCr_2O_4 in the spinel structure (space-group $Fd\bar{3}m$, $a = 8.31273\text{\AA}$ for $T = 15$ K) is the majority phase with a minority phase of 1% f. u. un-reacted Cr_2O_3 . Elastic and inelastic neutron scattering measurements were performed at NIST on the cold neutron triple-axis spectrometer SPINS. A vertically focusing Pyrolytic Graphite (002) monochromator (PG(002)) extracted a monochromatic beam with energy $2.5 \text{ meV} < E_i < 14 \text{ meV}$ from a ^{58}Ni coated cold neutron guide. The detection system consisted of a 20 cm long polycrystalline BeO filter cooled to 77 K followed by a 23 cm \times 15 cm flat PG(002) analyzer 92 cm from the sample, then a 80' radial collimator, and an area sensitive detector. The energy range detected was $2.6 \text{ meV} < E_f < 3.7 \text{ meV}$ with Full Width at Half Maximum (FWHM) energy resolution $0.1 \text{ meV} < \Delta E < 0.15 \text{ meV}$ and angular resolution $\Delta 2\theta \approx 50'$. The absolute efficiency of the instrument was measured using incoherent scattering from vanadium and nuclear Bragg peaks from ZnCr_2O_4 . The corresponding normalization factor was applied to background subtracted data to obtain measurements of the normalized magnetic neutron scattering intensity [12]

$$\tilde{I}(\mathbf{Q}, \omega) = \int \frac{d\Omega_{\hat{\mathbf{Q}}}}{4\pi} \left| \frac{g}{2} F(\mathbf{Q}) \right|^2 \sum_{\alpha\beta} (\delta_{\alpha\beta} - \hat{Q}_\alpha \hat{Q}_\beta) \mathcal{S}^{\alpha\beta}(\mathbf{Q}, \omega).$$

Here $F(Q)$ is the magnetic form factor for Cr^{3+} [13] and

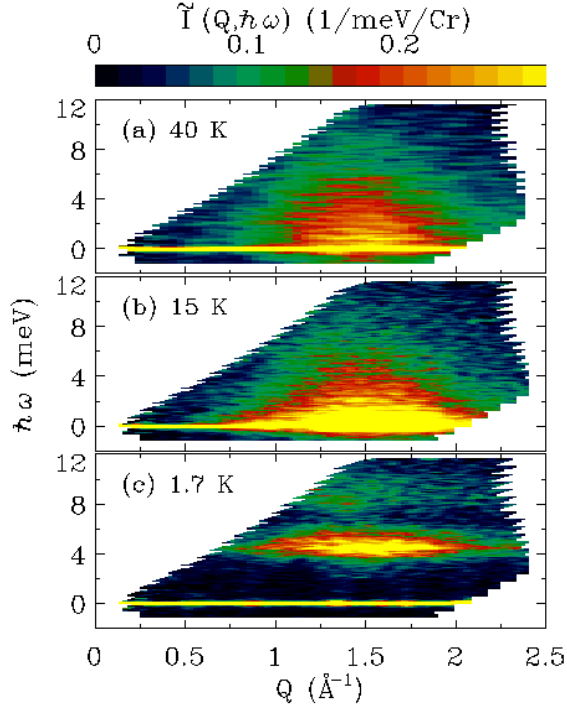


Fig. 1. Color maps of the magnetic neutron scattering intensity versus wave vector and energy transfer at three temperatures spanning the phase transition at $T_c = 12.5(5)$ K.

$S^{\alpha\beta}(\mathbf{Q}, \omega)$ is the scattering function [12].

Fig. 1 provides an overview of our data in the form of color images of $\tilde{I}(Q, \omega)$ at three temperatures. In the paramagnetic phase, Figs. 1 (a) and (b) provide evidence for quantum critical fluctuations of small AFM clusters most likely antiferromagnetically correlated tetrahedra. The data closely resemble those obtained in similar experiments on other frustrated AFM's [7,14]. For $T < T_c$ however, the low energy spectral weight concentrates into a sharp constant-energy mode centered at $\hbar\omega = 4.5$ meV $\approx |J| \gg k_B T_c$. Above the resonance there is an additional band of intensity centered at $\hbar\omega \approx 9$ meV (Fig. 2 (a)). Careful inspection of data below the resonance also reveals weak dispersing streaks emanating from AFM Bragg points.

Focusing first on the ordered phase, Fig. 2 (a) shows the Q -integrated magnetic scattering cross section at $T = 1.7$ K. With a resolution corrected FWHM of only 0.8 meV the $\hbar\omega = 4.5$ meV peak is evidence for a near dispersionless excitation. The spectral weight is $\hbar \int_{3.5\text{meV}}^{6\text{meV}} \sum_{\alpha\alpha} S^{\alpha\alpha}(\omega) d\omega = 0.59(1) / Cr$ which is 22% of the total fluctuating moment $((S(S+1) - |\langle \mathbf{S} \rangle|^2) = 2.65(5)/Cr)$ and corresponds to 16% of the total magnetic scattering cross section. Fig. 2 (b) shows the Q -dependence of the energy integrated intensity of this mode. The data exhibit a broad peak centered at $Q_0 = 1.5 \text{ \AA}^{-1}$ with a Half Width at Half Maximum

$\kappa = 0.48(5) \text{ \AA}^{-1} = 0.64(6)a^*$ indicating that the excited

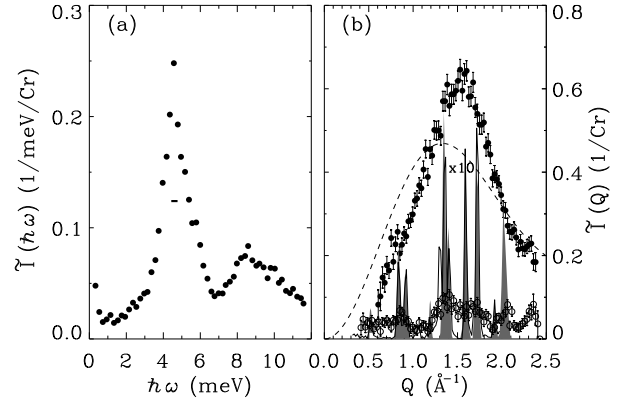


Fig. 2. Integrated magnetic scattering intensities at $T = 1.5$ K derived from Fig. 1 (c). (a) ω -dependence of the Q -integrated intensity: $\tilde{I}(\omega) = \int Q^2 dQ \tilde{I}(Q, \omega) / \int Q^2 dQ$. The horizontal bar shows the instrumental energy resolution. (b) Closed symbols show the Q -dependence of the ω -integrated resonance intensity: $\tilde{I}(Q) = \hbar \int_{3.5\text{meV}}^{6.0\text{meV}} \tilde{I}(Q, \omega) d\omega$. Open circles show data integrated from 1 meV to 3 meV. The solid line shows the elastic scattering cross section scaled by a factor 10. Shaded peaks are magnetic Bragg peaks.

state involves AFM correlated nearest neighbor spins. For comparison the dashed line shows the powder-averaged magnetic neutron scattering intensity for an isolated spin dimer at the nearest neighbor separation $r_0 = 2.939 \text{ \AA}$ [15]. The spin pair model produces a broader peak than the experiment indicating that the resonating spin cluster in ZnCr_2O_4 is more complex. Fig. 2 (b) also shows the wave vector dependence of inelastic scattering below the resonance integrated over energy from 1 meV to 3 meV (open symbols). Weak, non-resolution-limited peaks are visible and their locations coincide with AFM Bragg peaks (shaded). Excitations below the resonance are also apparent in the wave vector integrated data of Fig. 2 (a) where the intensity increases in proportion to energy for $\hbar\omega < 3.5$ meV (the low energy upturn is incompletely resolved elastic scattering). Both features are consistent with neutron scattering from spin waves in a three dimensional AFM powder with a spin gap $\Delta < 1.5$ meV. In particular the ratio of elastic to inelastic scattering is consistent with estimates based on spin wave theory in the long wavelength limit. From the width of the peaks we estimate a spin wave velocity $v = 18(2) \text{ meV\AA}$. This number is much less than the spin wave velocity for a bi-partite simple cubic AFM with $J = -2.8$ meV, $v = (2/\sqrt{3})z|J|sa = 239 \text{ meV\AA}$ but only slightly larger than the spin wave velocity for a cubic AFM with the critical temperature of ZnCr_2O_4 : $v = 2\sqrt{3}k_B T_c a / (S+1) = 12.4 \text{ meV\AA}$.

Spin wave theory provides a useful starting point for

understanding the resonance. Geometrical

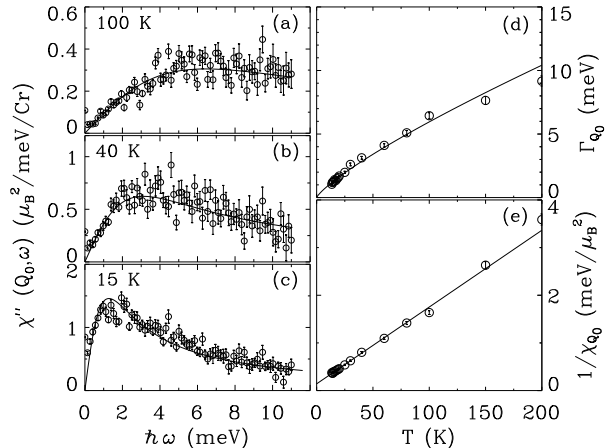


Fig. 3. (a)-(c) $\chi''(Q_0, \omega)$ at $Q_0 = 1.5\text{\AA}^{-1}$ derived from magnetic neutron scattering data via the fluctuation dissipation theorem. The solid lines are fits as described in the text. (d)-(e) Temperature dependence of the relaxation rate, $\Gamma_{Q_0}(T)$, and the inverse susceptibility, $\chi_{Q_0}^{-1}(T)$ derived from the fits.

frustration leads to constant energy surfaces or volumes for spin wave dispersion relations in reciprocal space. Such Q -space “degeneracy” in turn yields pronounced van-Hove singularities in wave vector averaged spectra. Reimers *et al* [16] showed that the pyrochlore AFM has two degenerate modes for any \mathbf{Q} in the Brillouin zone. Wave vector independent excitations also exist for the kagomé AFM [17] and these have a real space interpretation in terms of the so-called weather-vane modes [18]. A real-space interpretation has yet to be found for dispersionless excitations in the pyrochlore lattice. The broad peak in Fig. 2(b) indicates that they are highly localized in the ordered phase of ZnCr_2O_4 .

Turning now to excitations in the paramagnetic phase, Fig. 3 (a)-(c) show the imaginary part of the spin susceptibility, $\chi''(Q, \omega)$ for several temperatures larger than T_c . $\chi''(Q, \omega)$ was derived from inelastic neutron scattering data at $Q_0 = 1.5\text{\AA}^{-1}$ via the fluctuation dissipation theorem: $\chi''(Q, \omega) = (g\mu_B)^2\pi(1 - \exp(-\beta\omega))\mathcal{S}(Q, \omega)$. From the spectra we derived a temperature dependent spin relaxation rate, Γ_Q , and a static staggered susceptibility, χ_Q , by fitting to the following phenomenological response function: $\chi''(Q, \omega) = \chi_Q\Gamma_Q\omega/(\omega^2 + \Gamma_Q^2)$.

Figs. 3 (d) and (e) show the corresponding temperature dependent parameters. A power-law in T describes the temperature dependence of $\Gamma_{Q_0}(T) = \mathcal{C} \cdot k_B T (T/\theta)^{\alpha-1}$ for $T < 150$ K while $\chi_{Q_0}(T)$ can be described by a Curie-Weiss law: $\chi_{Q_0}(T) = (\mu_{Q_0}^2/3k_B\theta)1/(1 + T/\theta)$ in the entire temperature range. The best fit solid lines correspond to $\alpha = 0.81(4)$, $\mathcal{C} = 0.6(1)$, $\mu_{Q_0} = 4.0(1)\mu_B$, and $\theta = 8.8(4)$ K. Though we have plotted and analyzed data for $Q_0 = 1.5\text{\AA}^{-1}$ we found similar results for $\Gamma(T)$ in analysis of wave-vector

integrated data which probe the local spin susceptibility.

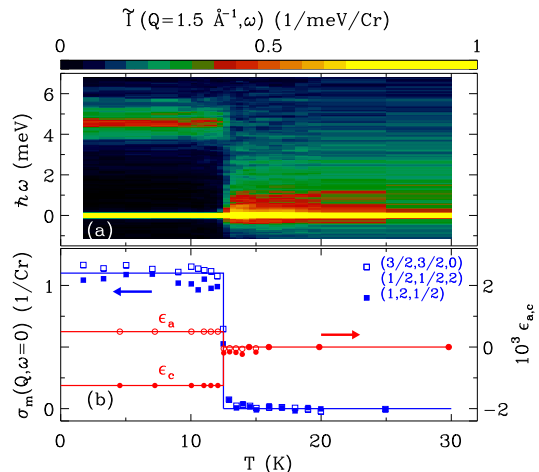


Fig. 4. (a) Color image of inelastic neutron scattering for $Q = 1.5\text{\AA}^{-1}$. (b) T -dependence of magnetic Bragg scattering from a powder (blue squares), $\sigma_m = \frac{v_m}{(2\pi)^3} \int \tilde{I}(Q, \omega) 4\pi Q^2 dQ d\hbar\omega$ where v_m is the volume per Cr^{3+} ion, and of lattice strain along \mathbf{a} and \mathbf{c} (red circles) measured by single crystal neutron diffraction.

At a quantum critical point, $k_B T$ is the only low energy scale for local response functions. If the lorentzian form for $\chi''(Q, \omega)$ describes the spectrum, then α must equal one at the critical point. This was the exponent found in Monte Carlo simulations of classical spins on a pyrochlore lattice [3]. The deviation of α from unity in ZnCr_2O_4 is perhaps not surprising given that the material does exhibit a magnetic phase transition. However, the fact that Γ_Q tends to zero as $T \rightarrow 0$ rather than at T_c indicates that the system may actually be approaching a quantum disordered phase with a gap $k_B\theta = 0.75$ meV before being interrupted by a first order transition to an unrelated competing phase. This idea is consistent with Fig. 4 which compares the temperature dependent lattice strain and magnetic Bragg peak intensity (frame (b)) to the inelastic neutron scattering spectrum at $Q_0 = 1.5\text{\AA}^{-1}$ (frame (a)). Magnetic Bragg peaks, a tetragonal lattice distortion, and the spin resonance all appear abruptly, and without conventional critical fluctuations at T_c .

Theoretical work has shown that magnetic order can not develop in an isotropic spin pyrochlore AFM [3,4]. There are many possible deviations from the perfect model that could cause ZnCr_2O_4 to order nonetheless. These include further neighbor interactions and spin space anisotropy [6,8,9]. Because the transition in ZnCr_2O_4 is of the first order and involves a lattice distortion, we suggest that finite lattice rigidity is an important factor at the phase transition in this material. Consider the effect of tetragonal strain on magnetism in ZnCr_2O_4 . It is well known that the exchange interaction between Cr^{3+} ions whose oxygen coordination octahe-

dra share an edge is strongly dependent on the Cr-Cr spacing, r [19]. Analysis of a series of chromium oxides indicates that $dJ/dr \approx 40$ meV/Å [20]. This implies that tetragonal strain $\epsilon_a > 0$ and $\epsilon_c < 0$ yields weaker AFM interactions in the basal plane, $\Delta J_{\perp} = r_0 \epsilon_a dJ/dr = 0.06$ meV, and stronger AFM interactions between all other spin pairs $\Delta J_{\parallel} = r_0(\epsilon_a + \epsilon_c)/2 dJ/dr = -0.04$ meV. This asymmetry reduces the mean field energy of the ordered phase in ZnCr_2O_4 by $\Delta\langle\overline{\mathcal{H}}_s\rangle = (5\Delta J_{\parallel} - \Delta J_{\perp})/2 \approx -0.07$ meV/Cr relative to the mean field ground state energy in the cubic phase [21]. The result should be Néel order in tetragonal ZnCr_2O_4 below an ordering temperature that we denote T_{Nt} . Because order appears abruptly and simultaneously with the tetragonal strain we infer that $T_{Nt} > T_c$. This may be possible despite the modest value of $\Delta\langle\overline{\mathcal{H}}_s\rangle$ because of the strong local constraints present when $|T/\Theta_{CW}| \ll 1$. In addition there could be other hitherto undetected lattice modifications at T_c that also favor Néel order (see below).

The magnitude of the lattice distortion is controlled by the need to balance the increase in lattice energy and the decrease in entropy against the decrease in the energy of the spin system. Equating the free energy $F = \langle\mathcal{H}_l + \mathcal{H}_s\rangle - TS$ of the competing phases at T_c implies that

$$\Delta\langle\mathcal{H}_s\rangle + \Delta\langle\mathcal{H}_l\rangle - T_c\Delta S = 0 \quad (1)$$

when cooling through T_c . We can derive $\Delta\langle\mathcal{H}_s\rangle$ from Fig. 1 (b) and (c) using the first moment sum rule: [22]

$$\Delta\langle\mathcal{H}_s\rangle = -\frac{3\hbar^2 \int_0^{\infty} \omega(1 - e^{-\beta\hbar\omega})\Delta\mathcal{S}(Q, \omega)d\omega}{2(1 - \sin Qr_0/QR_0)} \quad (2)$$

Limiting the integral to 0.2 meV to 12 meV and averaging data for $1.3 \text{ \AA}^{-1} < Q < 2 \text{ \AA}^{-1}$ yields a value of $\Delta\langle\mathcal{H}_s\rangle = -0.40(7)$ meV/Cr. From specific heat measurements [5] we find that $\Delta S = -0.107 R \ln 4/\text{Cr}$ corresponding to $-T_c\Delta S = 0.16$ meV/Cr. The difference between these numbers yields an estimate for the increase in lattice energy $\Delta\langle\mathcal{H}_l\rangle = 0.24(7)$ meV/Cr. The energy associated with simple tetragonal strain [23] only accounts for $v_0(c_{11}(\epsilon_c^2 + 2\epsilon_a^2)/2 + c_{12}(\epsilon_a^2 + 2\epsilon_a\epsilon_c)) = 0.026$ meV/Cr so there are likely additional modifications to the structure of ZnCr_2O_4 below T_c that help to stabilize Néel order.

There are interesting analogies between the phase transition in ZnCr_2O_4 and the spin-Peierls transition. In both cases the high T phase is near quantum critical and can lower its energy through a lattice distortion. In both cases the transition occurs from a strongly correlated paramagnet: $T_c \ll \Theta_{CW}$. And in both cases low energy spectral weight is moved into a finite energy peak. There are also important differences that render the transition in ZnCr_2O_4 a distinct new phenomenon in magnetism. The lattice distortion in ZnCr_2O_4 drives the spin system into an ordered phase not a quantum disordered phase. The transition in ZnCr_2O_4 is of the first order while the SP transition is of the second order. And the change in

entropy at T_c plays an important role in ZnCr_2O_4 , not in a SP transition. The central idea that finite lattice rigidity can drive a spin system away from quantum criticality however does carry over, and might be relevant for other frustrated magnets when symmetry breaking terms in the spin Hamiltonian fail to induce magnetic order.

We thank A. P. Ramirez for helpful discussions and for access to unpublished specific heat data. The NSF supported work at SPINS through DMR-9423101, work at JHU through DMR-9453362 and work at Rutgers through DMR-9802513.

* Present address: Francis Bitter Magnet Lab, Massachusetts Institute of Technology, Cambridge, MA 02139.

- [1] P. W. Anderson, Phys. Rev. **102**, 1008 (1956).
- [2] J. N. Reimers Phys. Rev. B **45** 7287 (1992).
- [3] R. Moessner and J.T. Chalker, Phys. Rev. Lett. **80**, 2929 (1998); Phys. Rev. B **57**, R5587 (1998) and Phys. Rev. B **58**, 12049 (1998).
- [4] B. Canals and C. Lacroix, Phys. Rev. Lett. **80**, 2933 (1998).
- [5] A.P. Ramirez, in “Magnetic Materials” to be published by North-Holland, Amsterdam (2000).
- [6] N. Raju *et al.*, Phys. Rev. B **59**, 14489 (1999).
- [7] J.S. Gardner *et al.*, Phys. Rev. Lett. **82**, 1012 (1999).
- [8] S.T. Bramwell, M.J.P. Gingras, and J.N. Reimers, J. Appl. Phys. **75**, 5523 (1994).
- [9] S. E. Palmer and J. T. Chalker, cond-mat/9912494 (1999).
- [10] G. G. P. Gorkom *et al.*, Phys. Rev. B **8**, 955 (1973).
- [11] J. C. M. Henning *et al.*, Phys. Rev. B **7**, 1825 (1973).
- [12] S.M. Lovesey, *Theory of Thermal Neutron Scattering from Condensed Matter*, (Clarendon Press, Oxford) 1984.
- [13] P. J. Brown, in “International Tables for Crystallography”, Volume C, edited by A. J. C. Wilson and E. Prince, Kluwer Academic Publishers Boston (1999).
- [14] S.-H. Lee *et al.*, Europhys. Lett. **35**(2), 127 (1996) and Phys. Rev. Lett. **76**, 4424 (1996).
- [15] A. Furrer and H. U. Güdel, J. Magn. Magn. Mater. **14**, 256 (1979).
- [16] J. N. Reimers *et al.*, Phys. Rev. B **43**, 865 (1991).
- [17] A. Chubukov, Phys. Rev. Lett. **69**, 832 (1992).
- [18] I. Ritchev *et al.*, Phys. Rev. B **47**, 15342 (1993).
- [19] J.B. Goodenough, Phys. Rev. **117**, 1442 (1960).
- [20] K. Motida and S. Miahara, J. Phys. Soc. Japan **28**, 1188 (1970).
- [21] A. Olés, Phys. Status Solidi A **3**, 569 (1970); H. Shaked *et al.*, Phys. Rev. B **1**, 3116 (1970); S.-H. Lee *et al.*, unpublished (1999).
- [22] P. C. Hohenberg and W. F. Brinkman, Phys. Rev. **10**, 128 (1974).
- [23] Y. Kino *et al.*, J. Phys. Soc. Japan **33**, 687 (1972).